

Research on Engineering Structures & Materials



www.jresm.org



Removal of cytotoxic tamoxifen from aqueous solutions with hydroxyapatite adsorbent

Serdar Çilenmez, Yavuz Ergün, İbrahim Bulduk

Online Publication Date: 30 February 2025

URL: http://www.jresm.org/archive/resm2025-598ma1227rs.html

DOI: http://dx.doi.org/10.17515/resm2025-598ma1227rs

Journal Abbreviation: Res. Eng. Struct. Mater.

To cite this article

Çilenmez S, Ergün Y, Bulduk İ. Removal of cytotoxic tamoxifen from aqueous solutions with hydroxyapatite adsorbent. *Res. Eng. Struct. Mater.*, 2025; 11(5): 2467-2480.

Disclaimer

All the opinions and statements expressed in the papers are on the responsibility of author(s) and are not to be regarded as those of the journal of Research on Engineering Structures and Materials (RESM) organization or related parties. The publishers make no warranty, explicit or implied, or make any representation with respect to the contents of any article will be complete or accurate or up to date. The accuracy of any instructions, equations, or other information should be independently verified. The publisher and related parties shall not be liable for any loss, actions, claims, proceedings, demand or costs or damages whatsoever or howsoever caused arising directly or indirectly in connection with use of the information given in the journal or related means.



Published articles are freely available to users under the terms of Creative Commons Attribution - NonCommercial 4.0 International Public License, as currently displayed at here (the "CC BY - NC").



Research on Engineering Structures & Materials



www.jresm.org

Research Article

Removal of cytotoxic tamoxifen from aqueous solutions with hydroxyapatite adsorbent

Serdar Çilenmez 1,a, Yavuz Ergün *,2,b, İbrahim Bulduk 3,c

- ¹Graduate School of Education Dept. of Energy and Environmental Sciences, Uşak University, Uşak, Türkiye
- ²Dept.of Chemical Eng., Faculty of Engineering and Natural Science, Uşak University, Uşak, Türkiye ³Dept. of Chemical Eng., Faculty of Engineering, Afyon Kocatepe University, Afyonkarahisar, Türkiye

Article Info

Abstract

Article History:

Received 27 Dec 2024 Accepted 25 Feb 2025

Keywords:

Wastewater; Tamoxifen; Removal; Hydroxyapatite; Adsorption The growing problem of pharmaceutical contamination poses a significant challenge to the protection of water resources. Tamoxifen, a widely used anticarcinogenic drug, is one of the pharmaceutical residues found in wastewater and poses serious environmental risks. In this study, chemically synthesized hydroxyapatite (HAP) was used as an adsorbent to remove tamoxifen from aqueous solutions. The synthesized HAP was thoroughly characterized by BET surface area analysis, SEM-EDX imaging and FTIR spectroscopy. A systematic evaluation of key adsorption parameters was carried out to determine the most effective conditions for tamoxifen removal. Experiments were performed by varying parameters such as initial tamoxifen concentration (20-70 µg/mL), solution pH (2-10), adsorbent dosage (20-50 mg per 50 mL solution), contact time (0-240 min) and temperature (298-318 K). The equilibrium state of the adsorption process was analyzed using Langmuir and Freundlich isotherm models. Pseudofirst and pseudo-second order kinetic models were used to determine the rate of the process. Thermodynamic properties were also calculated to provide information on the nature of the process. A maximum removal efficiency of 90.85% was obtained under optimum conditions of initial concentration 40 μg/mL, adsorbent dosage 40 mg, contact time 180 min and pH 7. Notably, the pseudo-second-order kinetic model (R2: 0.9997) and the Langmuir isotherm model (R²: 0.9994) exhibited the closest alignment with the experimental data. Thermodynamic studies have shown that the adsorption was a by itself ($\Delta G < 0$), exothermic ($\Delta H < 0$) process, accompanied by an increase in system disorder (Δ S>0). Consequently, this research underscores the viability of HAP as an economical and ecologically sound approach for remediating wastewater contaminated with pharmaceuticals.

© 2025 MIM Research Group. All rights reserved.

1. Introduction

Pharmaceutical compounds are chemicals widely used in the prevention, treatment, and diagnosis of diseases. However, through the pharmaceutical industry, hospital wastes, and domestic sewage, these compounds enter water resources and pose significant threats to the environment [1,2]. These chemicals damage the aquatic ecosystem and cause persistent pollution, leading to the development of resistant microorganisms and resistance genes. Moreover, due to their difficult biodegradation, these compounds are easily transported between water, soil, and living organisms and negatively affect human and animal health [3].

Tamoxifen, a powerful antiestrogen, is extensively utilized, particularly in the initial treatment and recurrence of breast cancer. Studies on its environmental effects reveal that this compound can

*Corresponding author: yavuz.ergun@usak.edu.tr

°orcid.org/0009-0007-9138-0190; °orcid.org/0000-0001-5883-2078; °orcid.org/0000-0001-6172-7738

DOI: http://dx.doi.org/10.17515/resm2025-598ma1227rs

Res. Eng. Struct. Mat. Vol. 11 Iss. 5 (2025) 2467-2480

negatively impact the reproductive abilities of aquatic organisms. It has been shown to disrupt vitellogenin levels in both female and male species, with generational impacts on their offspring [4]. Tamoxifen has been detected in varying concentrations in hospital wastewater, sewage, and surface waters [5–10], posing significant risks to aquatic ecosystems due to its toxicity, endocrine-disrupting properties, and bioaccumulation potential [11]. These findings highlight the importance of non-biological removal methods as an effective solution to eliminate tamoxifen from aquatic environments and prevent its atmospheric release. Nevertheless, research on the application of non-biological techniques for tamoxifen removal remains limited [12–16]. Therefore, further comprehensive studies are essential to explore alternative approaches for removing this anticancer drug from wastewater.

Pharmaceutical pollutants represent a significant threat to both ecosystems and human health due to their high-water solubility, persistence, and toxic characteristics [17,18]. To address this issue, various treatment methods have been developed, including biodegradation [19], advanced oxidation processes [20], photo-Fenton reactions [21], electro-Fenton systems [22], ozonation, membrane technologies [24], and adsorption techniques [25–27]. Among these, adsorption stands out as a particularly effective option, valued for its simplicity, high efficiency, and cost-effectiveness, especially in the removal of pharmaceutical compounds. In addition to traditional adsorbents like activated carbon, graphene oxide, zeolite, and clay, hydroxyapatite (HAP) has gained attention as an alternative due to its high adsorption capacity and biocompatibility. Adsorption is a versatile and promising technique, relying on the physical or chemical interaction of contaminants with the surface of the adsorbent. Compared to other methods, adsorption not only avoids the production of highly toxic by-products but also offers an efficient, low-cost solution for removing pharmaceutical compounds from wastewater [28–32].

Hydroxyapatite (HAP) has proven to be a highly effective adsorbent due to its unique properties. As a calcium phosphate compound with the chemical formula $Ca_{10}(PO_4)6(OH)_2$. HAP is widely recognized as a primary mineral component of bones and teeth. This remarkable material exhibits excellent biocompatibility, bioactivity, osteoconductivity, affinity, and nontoxicity. Its chemical and structural resemblance to the mineral constituents of human bones and teeth has made it a subject of extensive research over the years [33–37].

HAP's ability to accommodate a wide range of anionic and cationic substituents makes it versatile for various applications. It is commonly utilized in fields such as nanomedicine, drug and gene delivery, ion conduction, catalysis, biosensing, and tissue engineering. HAP can be obtained either synthetically or from natural sources, with numerous synthesis techniques documented in the literature. Synthetic HAP can be produced through a variety of methods, including dry processes (solid-state and mechanochemical synthesis), wet processes (chemical precipitation, hydrolysis, sol-gel, hydrothermal, emulsion, and sonochemical methods), and high-temperature techniques (combustion and pyrolysis) [38]. These diverse approaches enhance HAP's adaptability for specific applications, solidifying its importance across multiple scientific and industrial domains.

In this study, hydroxyapatite (HAP) adsorbents were synthesized using the sol-gel method and subsequently characterized. The potential of HAP for removing tamoxifen from wastewater was systematically evaluated. Adsorption kinetics were analyzed using pseudo-first-order and pseudo-second-order models, while adsorption equilibrium was studied through Langmuir and Freundlich isotherm models. Additionally, thermodynamic parameters were determined at 20, 30, and 40 °C to understand the nature of the adsorption process. To the best of our knowledge, this is the first report on the synthesis of HAP as an adsorbent and its application for the removal of pharmaceutical contaminants from aqueous solutions.

2. Materials and Methods

2.1. Tools, Chemicals and Materials

Tamoxifen levels in aqueous solutions were determined using an Agilent 1260 HPLC system (USA) with a UV detector and Chemstation software. pH measurements were taken with a Mettler-Toledo pH meter (Switzerland) using a glass electrode. All experiments utilized ultrapure water produced

by a Merck-Millipore Milli-Q system (USA), characterized by a conductivity below $0.05 \mu S/cm$ and a pH of 6.98, generated through reverse osmosis. Adsorption studies were performed in a WITEG WSB-30 shaking water bath (Germany) to maintain consistent experimental conditions.

Chemicals used included: ammonium phosphate dibasic ((NH₄)₂HPO₄, \geq 99.0%), calcium nitrate tetrahydrate (Ca(NO₃)₂·4H₂O, \geq 99.0%), sodium hydroxide (NaOH, 98%), hydrochloric acid (HCl, 37%), orthophosphoric acid (H₃PO₄, 85%), and potassium dihydrogen phosphate (KH2PO₄, \geq 99.0%). All chemicals were procured from Sigma-Aldrich Chemie (Istanbul, Turkey) and used as received. Tamoxifen (CAS No. 10540-29-01, C₂6H₂9NO, 99%) was purchased from Sigma-Aldrich Chemistry, and tamoxifen tablets (20 mg) were obtained from a local pharmacy in Afyonkarahisar, Turkey. Deionized water was used for all aqueous solutions, with pH adjustments made using HCl and NaOH to achieve the desired experimental conditions.

2.2. Hydroxyapatite (HAP) Synthesis

Natural bone consists of approximately 60 wt% amorphous or crystallized HAP, with a theoretical calcium-to-phosphorus (Ca/P) molar ratio of 1.67. This ratio was carefully considered during the synthesis of HAP via the sol-gel method. The synthesis began by dissolving 8.20 g of calcium nitrate tetrahydrate in 50 mL of ethanol. Simultaneously, 2.38 g of diammonium hydrogen orthophosphate was dissolved in 50 mL of double-distilled water. Both solutions were stirred continuously with a magnetic stirrer at 70 °C for 4 hours to ensure uniformity. After preparation, the solutions were allowed to hydrolyze for 24 hours. Subsequently, the diammonium hydrogen orthophosphate solution was gradually added to the calcium nitrate solution at a rate of 5 mL/min while stirring continuously at 36 °C for 4 hours to facilitate the reaction. The pH of the resulting mixture was adjusted to 7.4 using an ammonia solution.

In this supersaturated melt solution, nucleation occurs as the ions cluster and grow to a valid size. The crystals grow successively to form HAP, ranging in size from a few nanometers to $0.3~\mu m$. Grain growth in solution is dependent on concentration, time and temperature. As the formed HAP particles are covered with pore and film water, drying in an oven at $70~^{\circ}\text{C}$ for four hours and sintering at $800~^{\circ}\text{C}$ for one hour causes crystallization and grain growth. The removal of water by sintering causes the formation of heterogeneously grown crystals with a porous interconnected network as a result of the transformation into polycrystalline by the formation of an intergranular neck. The presence of impurities in the solution are factors affecting the formation and growth rate of the nucleus. The final product was stored in a sealed glass jar to preserve its integrity for subsequent adsorption studies.

2.3. Characterization Methods

To analyze the characteristics of the synthesized HAP, several techniques were used. Fourier Transform Infrared Spectroscopy (FTIR, Perkin Elmer) identified the surface functional groups. Brunauer-Emmett-Teller (BET) analysis, performed on a Micromeritics Gemini VII 5.03 system, determined the specific surface area and pore structure. Scanning Electron Microscopy (SEM, Zeiss Sigma 300) revealed the surface morphology, and Energy Dispersive X-ray (EDX) spectroscopy provided elemental composition data.

2.4. Determination of Zero Charge Point (pHpzc) of HAP Adsorbent

The pHpzc of HAP was determined by the salt addition technique. 1 liter of 0.1 M NaCl solution was prepared, and 50 mL volumes were taken into six different volumetric flasks; each of these volumes was transferred to 250 mL bottles. The initial pH value (pHi) of each volume was adjusted stepwise from 2 to 12 using 0.1 M hydrochloric acid (HCl) or 0.1 M sodium hydroxide (NaOH). Then, 0.050 g of HAP was added to each flask, and the mixtures were agitated at 25 °C and 170 rpm for 24 hours. After filtration, the final pH (pHf) of each filtrate was measured. A graph of pHi versus pHf was plotted, and the pHpzc was determined as the intersection point of the two curves [39].

2.5. Batch Adsorption Experiments

This study examined the effectiveness of utilizing HAP adsorbent to remove tamoxifen from aqueous solutions. The first step involved carefully weighing 50 mg of tamoxifen into a 100 mL

beaker, adding 40 mL of ultrapure water, and letting it dissolve. After the solution was moved to a $100\,\text{mL}$ volumetric flask, water was added to finish the volume. A stock solution containing $500\,\text{mg}$ mL-1 of tamoxifen was made. For five minutes, the stock solution was sonicated in an ultrasonic bath. $50\,\text{mL}$ tamoxifen solutions in $250\,\text{mL}$ capped Erlenmeyer flasks were used for the adsorption tests. The effects of variables such pH, adsorbent dosage, starting concentration, and temperature on the effectiveness of tamoxifen removal were assessed in adsorption experiments. To achieve the required concentrations for the set of tests, the stock solution was diluted. The solutions were shaken at $170\,\text{rpm}$ in a thermostatic water bath after the pH levels had been adjusted and the appropriate quantity of HAP adsorbent had been added. A $0.22\,\text{\mu m}$ membrane syringe filter was used to filter the samples, and an HPLC equipment was used to measure the amount of tamoxifen in the filtrates.

By adjusting pH between 2 and 10 while maintaining constant values for all other parameters, the impact of pH on the effectiveness of tamoxifen elimination was examined. Solutions of 0.1 N HCl or 0.1 N NaOH were used to alter the pH. Next, at the pH that provided the best clearance, the impact of various HAP dosages, ranging from 20 to 50 mg, on adsorption efficiency was assessed. Additionally, while holding other factors constant, the impact of temperature (293–313 K) and starting tamoxifen concentration (20–70 mg L^{-1}) on the removal efficiency was examined. A methodical assessment of the variables influencing adsorption efficiency was made possible by the triplicate execution of each experiment and the reporting of the average results. Equations 1 and 2 were used to determine the quantity of tamoxifen adsorbed per unit mass of HAP at a specific time t (qt) and equilibrium (qe):

$$qt = (Co-Ct)V/w (1)$$

$$qe = (Co - Ce)V/w (2)$$

Additionally, Equation 3 was used to determine the percentage of adsorbed tamoxifen:

$$Adsorption(\%) = \left(\frac{Co - Ce}{Co}\right) 100 \tag{3}$$

Where w (g) is the mass of HAP, V (L) is the volume of the solution, Ce (mg L⁻¹) is the equilibrium concentration, Ct (mg L⁻¹) is the concentration at time t, and C_0 (mg L⁻¹) is the initial concentration [40,41].

2.6. Equilibrium Modeling of Tamoxifen Removal Process

Adsorption isotherms are graphical representations that illustrate the relationship between the concentration of a substance in solution (adsorbate) and the amount of that substance adsorbed onto the surface of a material (adsorbent) at a constant temperature. These isotherms provide valuable insights into the nature of the interactions between the adsorbate and the adsorbent surface. In the context of this study, adsorption isotherms were used to model the interaction between tamoxifen and hydroxyapatite (HAP). By analyzing the equilibrium curves, researchers can understand how much tamoxifen is adsorbed onto the HAP surface at different concentrations, which is crucial for designing efficient adsorption systems. The Langmuir isotherm is a popular model that describes monolayer adsorption, where adsorbate molecules form a single layer on the adsorbent surface. It assumes that adsorption takes place at specific, identical sites on the surface, with each site accommodating only one adsorbate molecule. The linearized form of the Langmuir isotherm is given by Equation 4 [42]. By applying experimental data to this model, key parameters such as the maximum adsorption capacity (qmax) and the equilibrium constant (KL) can be determined. These parameters provide valuable information about the adsorption process and the interaction between tamoxifen and HAP.

$$\frac{Ce}{qe} = \frac{1}{qmKL} + Ce/qm \tag{4}$$

In this formula, qm stands for activated carbon's monolayer adsorption capacity (mg g^{-1}) and KL for the Langmuir adsorption constant (L mg^{-1}). The dimensionless separation factor (RL), which

shows if the adsorption procedure is feasible, can be used to assess the affinity between the adsorbent and the adsorbate. RL is computed using formula 5 as follows:

$$RL = 1/(1 + KLCo) \tag{5}$$

In this context, CoCo denotes the initial concentration of the adsorbate in the solution (mg L^{-1}). The RL value provides insight into the adsorption isotherm: When RL=0, adsorption is irreversible; when 0<RL<1, the isotherm is favorable for adsorption; when RL=1, the isotherm is linear; and when RL>1, the isotherm is unfavorable.

The Freundlich model differs from the Langmuir model in that it assumes the formation of multiple layers of adsorbate molecules on the adsorbent surface rather than a single homogeneous layer. This model is well-suited for describing adsorption on heterogeneous surfaces, where the adsorbent exhibits varying affinities for the adsorbate. The linearized form of the Freundlich isotherm model is represented by Equation 6 [43]:

$$In(qe) = In(KF) + \left(\frac{1}{n}\right)In(Ce) \tag{6}$$

In this equation, KF is the Freundlich constant (L mg^{-1}) and n is a parameter indicating the suitability of the adsorption process. If n > 1, higher concentrations should facilitate adsorbate adsorption on the adsorbent.

2.7. Kinetic Modeling of Tamoxifen Removal Process

The batch adsorption data were interpreted using pseudo-first-order and pseudo-second-order kinetic models and the corresponding kinetic parameters were calculated. The pseudo-first-order model assumes that each molecule of the adsorbate adheres to a specific site on the adsorbent and determines the adsorption rate depending on the sorption capacity of the solid surface. The linear form of this model is expressed as in equation 2.7 below [44,45]:

$$In(qe - qt) = In(qe) - k1t \tag{7}$$

In this equation, k1 is the pseudo-first-order rate constant (min⁻¹), and qe and qt indicate the adsorption capacities at equilibrium and at a specific time t (mg g⁻¹), respectively. On the other hand, the pseudo-second-order model explains the adsorption kinetics in relation to the adsorbent's capacity and is expressed by Equation 8.

$$\frac{t}{qt} = \frac{1}{k2qe^2} + \left(\frac{1}{qe}\right)t\tag{8}$$

This formula uses t as the elapsed time, k_2 as the pseudo-quadratic model's rate constant (g mg⁻¹ min⁻¹), and qe and qt as the adsorption capacities at equilibrium (mg g⁻¹).

2.8. Thermodynamic Modeling of Tamoxifen Removal Process

The spontaneity of the adsorption process and the impact of temperature on adsorption performance were assessed using thermodynamic metrics such as enthalpy (ΔH°), Gibbs free energy (ΔG°), and entropy (ΔS°) variations. Equation 9 [46] was used to determine the Gibbs free energy change (ΔG°):

$$\Delta G^{\circ} = -RT \ln(Ke) \tag{9}$$

The equilibrium constant, K_e , is defined by equation 2.10, the universal gas constant, R, is 8.314 J mol⁻¹ K⁻¹, and T is the absolute temperature (K).

$$Ke = \left(\frac{qe}{Ce}\right) \tag{10}$$

Where Ce and qe are the equilibrium concentrations of tamoxifen in solution (mg L-1) and on the adsorbent (mg g-1), respectively. The relationship between ΔG° , ΔH° and ΔS° is expressed as follows 11:

$$\Delta G^{\circ} = \Delta H^{\circ} - T \Delta S^{\circ} \tag{11}$$

Rearranging this expression leads to a linear equation 2.12 that allows the calculation of thermodynamic parameters:

$$In(Ke) = \left(\frac{\Delta S^{\circ}}{R}\right) - \left(\frac{\Delta H^{\circ}}{RT}\right) \tag{12}$$

2.9. Quantification of Tamoxifen in Aqueous Solutions

Using a 1260 Infinity LC system (Agilent, USA) and high-performance liquid chromatography (HPLC), the amount of tamoxifen in the solutions was determined. An ODS-3 C18 chromatographic column (250 × 4.6 mm, 5 μ m) was used for separation, and a wavelength of 278 nm was used for detection. A mobile phase comprising a 50:50 (v/v) ratio of acetonitrile and 0.01 M KH₂PO₄ solution (pH:2, adjusted with phosphoric acid) was used to conduct the analysis under isocratic conditions. The injection volume was 5 μ L, the flow rate was 1.0 mL min⁻¹, and the column temperature was kept at 30 °C.

3. Results and Discussion

3.1. Characterization of HAP

SEM, FTIR, and XRD analyses were used to describe the HAP samples. To examine the surface morphology of HAP, SEM was employed. Figures 1a and 1b display SEM pictures of HAP in the form of polycrystalline bonds. It had a porous structure that varied in size. The results of earlier research on HAP are in line with this extremely porous material [47]. The specific properties, morphology, porosity, pore size, surface area, polarity and stiffness of sol-gel obtained HAPs are largely dependent on the progress of the hydrolysis and condensation reactions and are also influenced by the choice of precursor, water-precursor molar ratio, solvent and co-solvent, pressure, temperature, ageing, drying and sintering conditions.

The structure of HAP was ascertained by FTIR analysis, and the resulting spectrum is shown in Figure 1d. The OH stretching vibrations of the surface P-OH groups were identified as the source of a faint signal at 3670 cm⁻¹ in the FTIR spectrum. The stretching vibration of lattice OH ions is identified by a distinct band at 3572 cm⁻¹. The overtone and combination bands of PO_3^{-4} ions are shown by three bands at 2142, 2077, and 1989 cm⁻¹. The OH-O bands of adsorbed water and the HAP of P-O attached to PO_3^{-4} groups are characterized by low-intensity, poorly defined absorption bands in the 1080-1020 cm⁻¹ area. Around 600-610 cm⁻¹, there is a distinct peak that is indicative of the O-H vibrational mode. The CO_2^{-3} groups are represented by the bands in the 1380-1580 cm⁻¹ range. PO_3^{-4} is responsible for the bands at 900-1300 cm⁻¹ [47].

Figure 2a shows the XRD image obtained from HAP samples. As seen intensely in the standard peak of HAP, the approximate 20 angles of 100%, 63% and 52% peaks vary between $\approx 31\text{-}33^\circ$. The reflection planes from these angles are distributed in the region between (211) - (300) and (112) respectively. The identified planes were determined by reflection (diffraction) from the lattice parameters of the synthesized HAP samples. Unlike standard HAP, only very little β TCP and trace CaO phases were found. β TCP does not pose any disadvantage in terms of biocompatibility [48]. Nowadays, it has been found that compounds containing calcium phosphate ceramics with a mixture of HA and β TCP give much better results compared to single phase HAP and β TCP [49,50]. The presence of CaO phase may have been formed by the replacement of carbonate groups stabilized in the natural hydroxyl region with OH in the HAP structure [50]. It is seen that the phases obtained from the samples by XRD are very close to the standard phase and the degree of crystallization is quite high with the absence of unwanted phases and the peak intensities obtained are very strong.

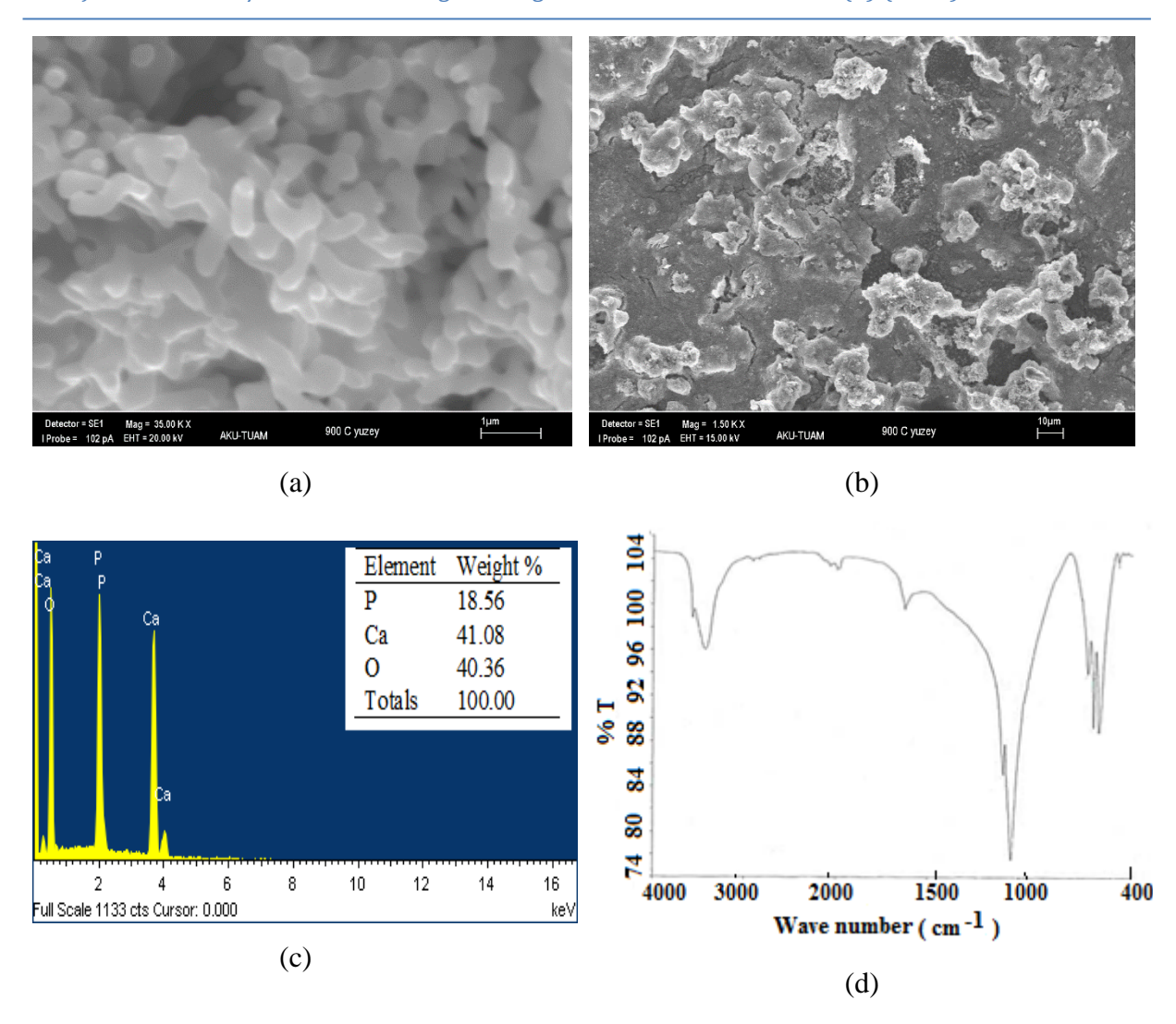


Fig. 1. (a) and (b) SEM images of HAP at various magnification levels (A: 1 μ m, B: 10 μ m), (c) EDX image and elemental composition of HAP, and (d) FTIR spectrum of HAP

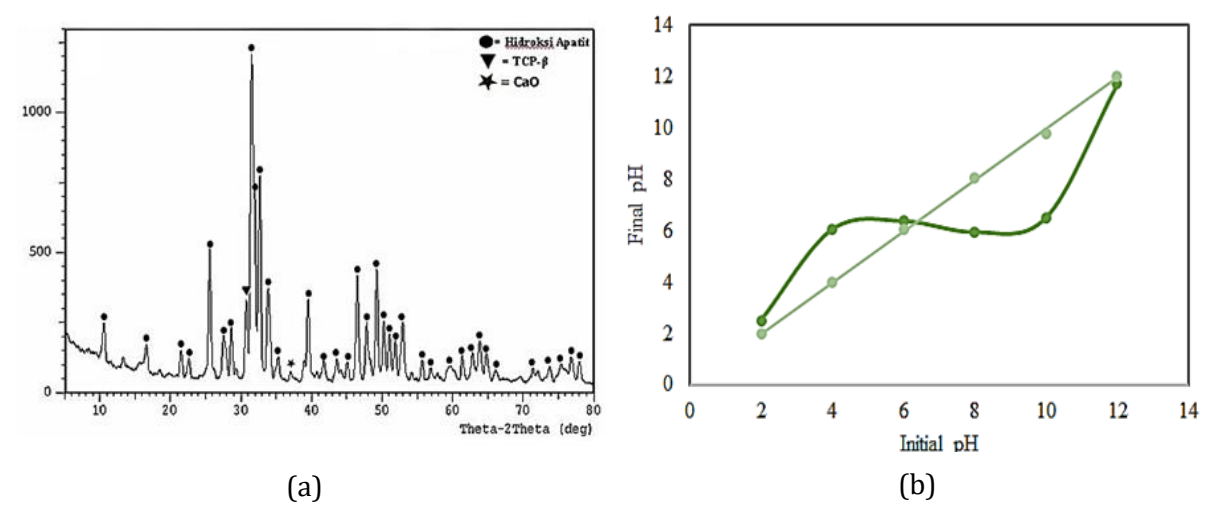


Fig. 2. (a) XRD image of HAPand (b) pHPZC graph

3.2. Determination of pHpzc of HAP

The pHpzc signifies the pH where an adsorbent's surface carries a net neutral charge. This metric is crucial for interpreting electrostatic forces that govern interactions of the adsorbent and adsorbate at varying pH conditions. As depicted in Figure 2b, the pHpzc for HAP is 6.10. Below this pH, the surface of the adsorbent exhibits a positive charge, thereby enhancing its ability to attract

anions. Conversely, at pH levels exceeding the pHpzc, the surface acquires a negative charge, favoring the adsorption of cations [45]. This trend, where the surface charge transitions to negative above pH 6.10, aligns with the behavior observed in activated carbon, which also demonstrates a negative zeta potential under similar conditions.

3.3. Effect of pH on Tamoxifen Removal Efficiency

Five solutions with a concentration of 50 mg L^{-1} and pH values ranging from 2 to 10 were made in order to investigate the impact of pH on adsorption efficiency. Each sample was treated with 40 mg of weighed adsorbent. Following this procedure, the samples were kept in the mixer for three hours at a speed of 170 rpm and an ambient temperature of 25 °C. The HPLC system was used to evaluate the samples that were collected at the conclusion of the time. Figure 3a presents the findings. Figure 3a in this investigation shows that tamoxifen adsorption rose when solution pH rose to a value of 6. From pH 2 to pH 6, the elimination efficiency rose linearly, from 68.88% to 93.63%. The elimination efficiency then declined as the pH value dropped.

3.4. Effect of Adsorbent Dose on Tamoxifen Removal Efficiency

Six solutions with a concentration of $40~mg~L^{-1}$ and pH 7 were prepared and the effect of the amount of adsorbent used on the efficiency of adsorption has been studied. Different amounts of adsorbents were weighed and added to each solution. The mixtures were shaken on a shaker at 170 rpm stirring speed and 25 °C ambient temperature for 120 min. Two milliliters of solution were drawn into the syringe and filtered into the HPLC vial using a syringe tip filter. Quantification analysis was performed on the HPLC system. Figure 3b shows the change in the adsorption efficiency of the amount of adsorbent with the amount of adsorbent.

Figure 3b illustrates how the clearance efficiency of tamoxifen rises as the dosage amount does. The efficiency in the study, which began with a dose of 20 mg, was 82.90%. At a dose of 40 mg, the removal efficiency increased to about 92.05% by increasing the adsorbent dose. The improvement in removal efficiency can be considered linear up to a dose of 40 mg. The efficiency was determined to be 94.48% in the 50 mg dose study and 95.45% in the 60 mg dose research. The elimination efficiency did not significantly alter after 50 mg, and the graph kept moving horizontally. At 60 mg, the adsorbent dosage achieved 95.45% efficiency. Lastly, a dose of 70 mg produced an efficiency of 95.55%. Although saturation was attained and the efficiency at 50 mg dose was 94.48%, Figure 2b shows that the ideal dose to use the least amount of adsorbent and attain an adsorption efficiency above 90% was 40 mg.

3.5. Effect of Stirring Time on Tamoxifen Removal Efficiency

30 mg of HAP adsorbent was added to tamoxifen solution at an initial concentration of 40 mg L⁻¹ with pH 7 at 25 °C, and the mixture was shaken at 170 rpm for 240 minutes in order to examine the impact of stirring duration on adsorption efficiency. An injector was used to sample 1 mL of the solution at predetermined intervals, filter it via a vial equipped with an injector tip filter, and then analyze it in an HPLC system. Figure 3c shows how the adsorption effectiveness changes with stirring time.

Up to 30 minutes, the adsorption efficiency is shown to grow linearly with an increase in stirring time; beyond that, there is a minor increase in removal efficiency between 30 and 60 minutes, after which it becomes almost constant. The efficiency in the 30-minute contact time study was 65.63%. Contact time was 86.48% at 120 minutes, and equilibrium with a yield of 90.85% was established after 180 minutes. Consequently, 180 minutes was determined to be the ideal duration for the subsequent investigation and equilibrium adsorption kinetic modeling. As a consequence, 91.60% efficiency was attained after 240 minutes of equilibrium. These findings led to the conclusion that 180 minutes was the ideal mixing period.

3.6. Effect of Initial Tamoxifen Concentration on Removal Efficiency

Tests were performed at pH 7, temperature 25 $^{\circ}$ C, stirring period 180 min, adsorbent amount 40 mg in 50 mL, initial concentration 20-70 mg L⁻¹, and to examine the impact of initial concentration on the elimination of tamoxifen. Based on the findings, it was concluded that the starting

concentration affected the adsorption of tamoxifen. The impact of the baseline tamoxifen concentration on the removal level is given in Figure 3d.

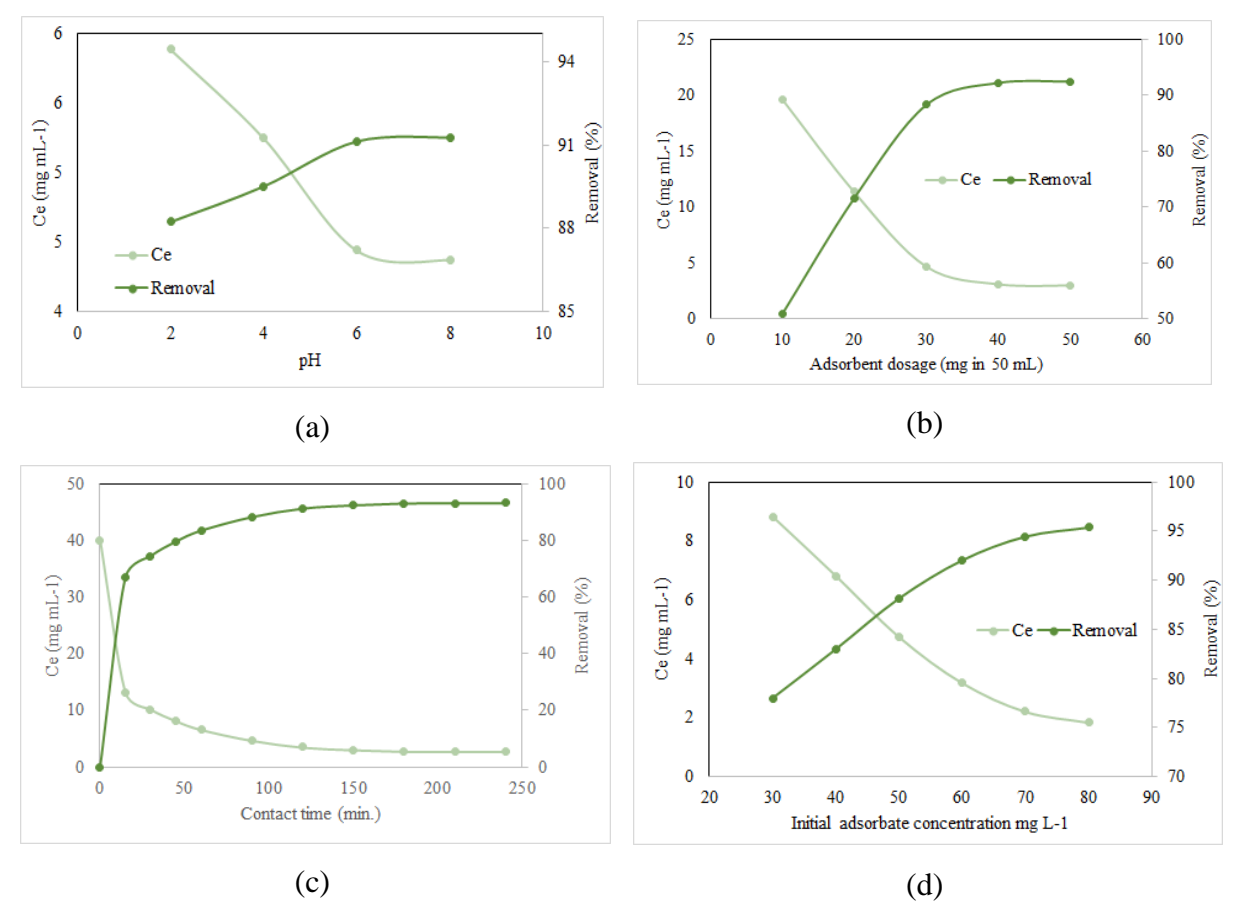


Fig. 3. (a) pH's impact on the effectiveness of tamoxifen elimination, (b) The impact of asorbent dose on the effectiveness of tamoxifen elimination, (c) The impact of stirring duration on the effectiveness of tamoxifen elimination, and (d) The impact of starting concentration on the effectiveness of tamoxifen elimination

The elimination of tamoxifen changes with increasing concentration, as seen in Figure 3D. When the concentration was 20 mg L-1, the clearance efficiency was 82.90%; at 30 mg L-1, it was 88.05%; and at 40 mg L-1, it was 92.05%. In this concentration range, a notable improvement in removal efficiency was noted. At concentrations higher than the initial 40 mg L-1 concentration, no discernible improvement in removal efficiency was seen. The elimination efficiency was 94.48% at a concentration of 50 mg L-1, 95.45% at 150 mg L-1, and 95.55% at 70 mg L-1. This is to be expected as tamoxifen retention by the adsorbent diminishes with saturation. These findings led to the conclusion that 40 mg L-1 was the ideal starting concentration.

3.7. Effect of Ambient Temperature on Tamoxifen Removal Efficiency

To determine temperature impact on the adsorption process, the temperature was 25 °C, the stirring time was 180 min, the pH of the tamoxifen solution with a volume of 50 mL and an initial concentration of 40 mg L^{-1} was adjusted to 7.00 and 40 mg of adsorbent was added and experiments were carried out. Experimental studies were carried out at 25 °C, 35 °C and 45 °C. The effect of temperature on tamoxifen removal efficiency is presented in Figure 4.

When Figure 4 is examined, it is observed that 90.85% efficiency was achieved at 25 °C. As the temperature increased, the efficiency gradually decreased, dropping to 78.98% at 45 °C. The findings reveal that an increase in temperature reduces adsorption efficiency, indicating that the process is exothermic. Furthermore, it was observed that an increase in temperature negatively affected diffusion within the adsorbent by lowering the solution viscosity. Compared with similar studies in the literature, it was found that the results of this study are consistent with the literature

and that the temperature increase similarly reduced efficiency. In light of all these evaluations, it is concluded that temperature variation affects the adsorption equilibrium capacity.

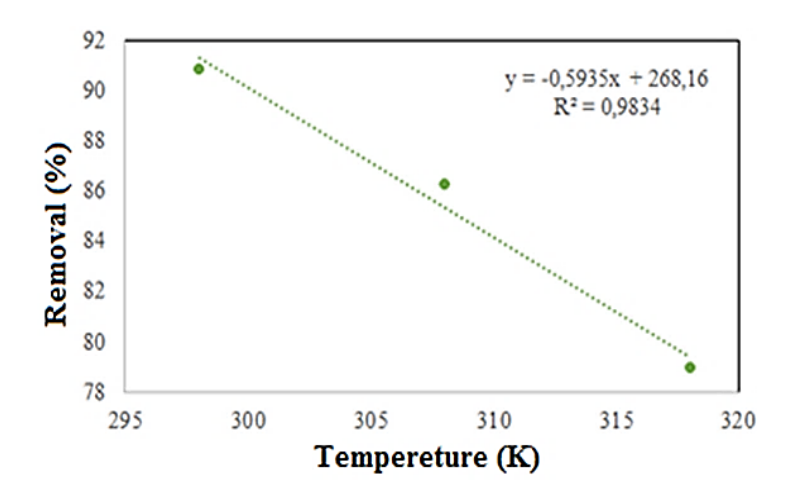


Fig. 4. Effect of temperature on tamoxifen removal efficiency

3.8. Adsorption Thermodynamics

The adsorption process was analyzed thermodynamically by calculating the enthalpy (ΔH), entropy (ΔS), Gibbs free energy change (ΔG), and equilibrium constant (K). Temperature was a critical factor in this study. Using 40 mg of adsorbent and a tamoxifen solution with a concentration of 40 mg L⁻¹, trials were conducted at three temperatures (25 °C, 35 °C, and 45 °C) to investigate the impact of temperature on tamoxifen adsorption. The equilibrium constants (K) were determined for each temperature, and the corresponding ΔG values were derived. The ΔH and ΔS values were calculated using the slope of the linear relationship between 1/T and lnK. The resulting thermodynamic parameters for tamoxifen adsorption are presented in Table 1.

Table 1. Thermodynamic parameters for tamoxifen adsorption

Temperature (K)	ΔG (J mol ⁻¹)	ΔH (J mol ⁻¹)	ΔS (J mol ⁻¹)	
298	-70.225			
308	-71.298	-34.442	107	
318	-72.371	-34.442	107	

The standard free energy change (ΔG) was negative across all temperature conditions, confirming that the adsorption process is spontaneous [47]. As illustrated in Table 2, the free energy change of adsorption becomes less negative with increasing temperature, suggesting that adsorption is more efficient at lower temperatures. In tamoxifen adsorption, higher temperatures reduced the adsorption efficiency. The negative ΔH value indicates that the process is exothermic, and the positive ΔS value points to an increase in system disorder during adsorption.

3.9. Adsorption Isotherms

To elucidate the adsorption mechanism of tamoxifen onto HAP, the experimental results were subjected to analysis using both Langmuir and Freundlich isotherm models. The parameters derived from these models are compiled in Table 2. The accuracy of the models was assessed by their respective correlation coefficients (R^2), revealing that the Langmuir model demonstrated a superior fit to the experimental data. The Langmuir model, which posits a monolayer and uniform adsorption process, proved to be more representative of the observed data. Conversely, the Freundlich model exhibited a poorer fit, reflected in a diminished R^2 value. The strong correlation coefficient ($R^2 = 0.9994$) obtained from the Langmuir model substantiates the notion that tamoxifen adsorption on HAP occurs as a monolayer, with the adsorbent possessing evenly distributed active sites and consistent binding interactions [48]. The maximum theoretical

adsorption capacity (q_{max}) determined by the Langmuir model serves as a crucial metric for designing methods for efficient adsorption for specific contaminants, and it is closely aligned with the experimentally determined equilibrium capacity values (Table 2). While the Freundlich model yielded comparatively lower R^2 values, the factor affecting heterogeneity (n) exceeded 1, signifying a favorable adsorption process [49]. Nevertheless, due to the diminished agreement between the experimental data and the Freundlich model, a lower R^2 value resulted. Furthermore, the R_L constant, calculated to be 0.1930, indicated a strong adherence to this isotherm, as R_L values within the range of 0 to 1 suggest favorable adsorption. Additionally, the elevated K_L value, which signifies the affinity of tamoxifen for HAP, further reinforces the suitability of the Langmuir isotherm for the data [50].

Table 2. Important parameters of Langmuir and Freundlich isotherm models

Langmuir isotherm model data			Freundlich isotherm model data		
q _{max} (mg g ⁻¹)	K_L (mgL ⁻¹)	\mathbb{R}^2	$K_F (mg g^{-1})$	n	\mathbb{R}^2
43.48	41.818	0.9994	31.00	5.17	0.7117

3.10. Adsorption Kinetics

To understand the rate of the adsorption process, PFO and PSO kinetic models were employed. The associated set of kinetic parameters and their correlation coefficients are detailed in Table 3. The PFO model implies that adsorption is governed by diffusion through a boundary layer, whereas the PSO model indicates that the main process is chemical adsorption. [51]. Upon examination of the data in the table, it becomes clear that tamoxifen adsorption aligns closer with the PSO model. This is proven by the higher correlation coefficient ($R^2 = 0.9997$) obtained for the PSO model compared to the PFO model ($R^2 = 0.8660$). Additionally, the experimentally observed adsorption capacity (qe = 45.80 mg g⁻¹) closely matched the calculated capacity from the PSO model (qe = 47.62 mg g⁻¹), further validating the PSO model's applicability. Consequently, it can be confidently stated that chemical adsorption is the predominant mechanism for tamoxifen adsorption onto the adsorbent surface.

Table 3. Important parameters of the pseudo-first order (PFO) and pseudo-second order (PSO) models

Pseudo-first-order kinetic model data			Pseudo- second-order kinetic model data		
k1 (min -1)	qe (mg g-1)	R2	k2 (g mg-1 min-1)	qe (mg g-1)	R2
0.0282	33.00	0.8660	0.0022	47.62	0.9997

4. Discussion

The results of this study show that hydroxyapatite (HAP) produced by the Sol-gel method can be used as a successful adsorbent for the effective removal of tamoxifen from synthetic wastewater. The optimum conditions obtained ($40 \,\mu\text{g/mL}$ initial concentration, $25\,^{\circ}\text{C}$ temperature, pH 7, $40 \,\text{mg}$ HAP dose per 50 mL solution, and 180 min contact time) provided a high efficiency of 90.85% for tamoxifen removal. The high agreement of the measurement values with the Langmuir isotherm model (R^2 : 0.9994) indicates that adsorption occurs on monolayer and homogeneous surfaces. This suggests that the HAP surface has a monolayer structure capable of strong interactions with tamoxifen molecules. On the other hand, the fit of the pseudo-second-order kinetic model (R^2 : 0.9997) indicates that chemical bonds are at the forefront in the adsorption process and HAP forms specific bonds with tamoxifen molecules. This finding suggests that the chemical properties of HAP may play an important role in the treatment of pharmaceutical compounds.

Thermodynamic analyses showed that the adsorption of tamoxifen on HAP is a by itself ($\Delta G < 0$), exothermic ($\Delta H < 0$) process characterized by entropy increase ($\Delta S > 0$). These results confirm that low temperatures increase tamoxifen removal and that the adsorption has an exothermic nature.

Since exothermic processes are more efficient at low temperatures, this result suggests that HAP can also reduce energy costs in the treatment of wastewater containing tamoxifen. This study makes an important contribution that tamoxifen should be removed with strong adsorbents such as HAPs due to its difficult biodegradation and high toxicity. Conventional methods often result in low efficiency and can produce toxic by-products. The high adsorption capacity, biocompatibility, low cost, and non-toxic nature of HAP make it an environmentally friendly option. In the studies available in the literature, tamoxifen is usually reported to be removed by adsorbents such as activated carbon; however, the high efficiency of HAP demonstrated in this study suggests that HAP may be an important alternative in this field.

In conclusion, the high performance of HAP produced by the Sol-Gel method in tamoxifen removal confirms that this adsorbent offers a potential solution for the removal of pharmaceutical impurities. This study demonstrated that HAP is an effective approach for the treatment of difficult-to-remove pharmaceutical contaminants such as tamoxifen, especially from the pharmaceutical industry and hospital wastewater. In the future, investigating the effects of HAP on other pharmaceutical compounds and environmental pollutants will provide important insights into how this method can be optimized in larger-scale applications. In this context, further studies testing the applicability of HAP in different wastewater matrices could further elucidate the potential of this adsorbent in industrial treatment processes.

References

- [1] Lung I, Soran ML, Stegarescu A, Opris O, Gutoiu S, Leostean C, Lazar MD, Kacso I, Silipas TD, Porav AS. Evaluation of CNT-OOH/MnO2/Fe3O4 nanocomposite for ibuprofen and paracetamol removal from aqueous solutions. J Hazard Mater. 2021;403:123528. https://doi.org/10.1016/j.ihazmat.2020.123528
- [2] Alothman ZA, Badjah AY, Alharbi OML, Ali I. Copper carboxymethyl cellulose nanoparticles for efficient removal of tetracycline antibiotics in water. Environ Sci Pollut Res Int. 2020;27(32):42960-42968. https://doi.org/10.1007/s11356-020-10189-1
- [3] Zandipak R, Sobhanardakani S. Novel mesoporous Fe304/Si02/CTAB-Si02 as an effective adsorbent for the removal of amoxicillin and tetracycline from water. Clean Technol Environ Policy. 2018;20(4):871-885. https://doi.org/10.1007/s10098-018-1507-5
- [4] Li J, Yu G, Pan L, Li C, You F, Xie S, Wang Y, Ma J, Shang X. Study of ciprofloxacin removal by biochar obtained from used tea leaves. J Environ Sci (China). 2018;73:20-30. https://doi.org/10.1016/j.jes.2017.12.024
- [5] Sun L, Zha J, Spear AP, Wang Z. Tamoxifen effects on the early life stages and reproduction of Japanese medaka (Oryzias latipes). Environ Toxicol Pharmacol. 2007;24(1):23-29. https://doi.org/10.1016/j.etap.2007.01.003
- [6] Roberts PH, Thomas KV. The occurrence of selected pharmaceuticals in wastewater effluent and surface waters of the lower Tyne catchment. Sci Total Environ. 2006;356:143-153. https://doi.org/10.1016/j.scitotenv.2005.04.031
- [7] Besse JP, Latour JF, Garric J. Anticancer drugs in surface waters: what can we say about the occurrence and environmental significance of cytotoxic, cytostatic and endocrine therapy drugs? Environ Int. 2012;39(1):73-86. https://doi.org/10.1016/j.envint.2011.10.002
- [8] Ashton D, Hilton M, Thomas KV. Investigating the environmental transport of human pharmaceuticals to streams in the United Kingdom. Sci Total Environ. 2004;333:167-184. https://doi.org/10.1016/j.scitotenv.2004.04.062
- [9] Ferrando-Climent L, Cruz-Morató C, Marco-Urrea E, Vicent T, Sarrà M, Rodriguez-Mozaz S, Barceló D. Nonconventional biological treatment based on Trametes versicolor for the elimination of recalcitrant anticancer drugs in hospital wastewater. Chemosphere. 2015;136:9-19. https://doi.org/10.1016/j.chemosphere.2015.03.051
- [10] Ferrando-Climent L, Rodriguez-Mozaz S, Barceló D. Development of a UPLC-MS/MS method for the determination of 10 anticancer drugs in hospital and urban wastewaters, and its application for the screening of human metabolites assisted by information-dependent acquisition tool (IDA) in sewage samples. Anal Bioanal Chem. 2013;405(19):5937-5952. https://doi.org/10.1007/s00216-013-6794-4
- [11] Ferrando-Climent L, Rodriguez-Mozaz S, Barceló D. Incidence of anticancer drugs in an aquatic urban system: from hospital effluents through urban wastewater to the natural environment. Environ Pollut. 2014;193:216-23. https://doi.org/10.1016/j.envpol.2014.07.002
- [12] Jean J, Perrodin Y, Pivot C, Trepo D, Perraud M, Droguet J, et al. Identification and prioritization of bioaccumulable pharmaceutical substances discharged in hospital effluents. J Environ Manage. 2012;103:113-21. https://doi.org/10.1016/j.jenvman.2012.03.005

- [13] DellaGreca M, Iesce MR, Isidori M, Nardelli A, Previtera L, Rubino M. Phototransformation products of tamoxifen by sunlight in water. Toxicity of the drug and its derivatives on aquatic organisms. Chemosphere. 2007;67(10):1933-9. https://doi.org/10.1016/j.chemosphere.2006.12.001
- [14] Chen Z, Park G, Herckes P, Westerhoff P. Physicochemical treatment of three chemotherapy drugs: irinotecan, tamoxifen, and cyclophosphamide. J Adv Oxid Technol. 2008;11(2):254-60. https://doi.org/10.1515/jaots-2008-0209
- [15] Zhang J, Chang VWC, Giannis A, Wang JY. Removal of cytostatic drugs from the aquatic environment: a review. Sci Total Environ. 2013;445-6:281-98. https://doi.org/10.1016/j.scitotenv.2012.12.061
- [16] Negreira N, Regueiro J, López de Alda M, Barceló D. Transformation of tamoxifen and its major metabolites during water chlorination: identification and in silico toxicity assessment of their disinfection byproducts. Water Res. 2015;85:199-207. https://doi.org/10.1016/j.watres.2015.08.036
- [17] Ferrando-Climent L, Gonzalez-Olmos R, Anfruns A, Aymerich I, Corominas L, Barceló D, et al. Elimination study of the chemotherapy drug tamoxifen by different advanced oxidation processes: transformation products and toxicity assessment. Chemosphere. 2017;168:284-92. https://doi.org/10.1016/j.chemosphere.2016.10.057
- [18] Zhou Y, He Y, Liu X, Xu B, Yu J, et al. Analyses of tetracycline adsorption on alkali-acid modified magnetic biochar: site energy distribution consideration. Sci Total Environ. 2019;650:2260-6. https://doi.org/10.1016/j.scitotenv.2018.09.393
- [19] Shao S, Hu Y, Cheng J, Chen Y. Biodegradation mechanism of tetracycline (TEC) by strain Klebsiella sp. SQY5 as revealed through products analysis and genomics. Ecotoxicol Environ Saf. 2019;185:109676. https://doi.org/10.1016/j.ecoenv.2019.109676
- [20] Li C, Lin H, Armutlulu A, Xie R, Zhang Y, Meng X. Hydroxylamine-assisted catalytic degradation of ciprofloxacin in ferrate/persulfate system. Chem Eng J. 2019;360:612-20. https://doi.org/10.1016/j.cei.2018.11.218
- [21] Yi H, Lai C, Huo X, Qin L, Fu Y, Liu S, et al. $\rm H_2O_2$ -free photo-Fenton system for antibiotics degradation in water via the synergism of oxygen-enriched graphitic carbon nitride polymer and nano manganese ferrite. Environ Sci Nano. 2022;9:815-26. https://doi.org/10.1039/D1EN00869B
- [22] Shoorangiz M, Nikoo MR, Salari M, Rakhshandehroo GR, Sadegh M. Optimized electro-Fenton process with sacrificial stainless steel anode for degradation/mineralization of ciprofloxacin. Process Saf Environ Prot. 2019;132:340-50. https://doi.org/10.1016/j.psep.2019.10.011
- [23] Hassani A, Khataee A, Fathinia M, Karaca S. Photocatalytic ozonation of ciprofloxacin from aqueous solution using TiO₂/MMT nanocomposite: nonlinear modeling and optimization of the process via artificial neural network integrated genetic algorithm. Process Saf Environ Prot. 2018;116:365-76. https://doi.org/10.1016/j.psep.2018.03.013
- [24] Palacio DA, Leiton LM, Urbano BF, Rivas BL. Tetracycline removal by polyelectrolyte copolymers in conjunction with ultrafiltration membranes through liquid-phase polymer-based retention. Environ Res. 2020;182:109014. https://doi.org/10.1016/j.envres.2019.109014
- [25] Liu J, Zhou B, Zhang H, Ma J, Mu B, Zhang W. A novel biochar modified by chitosan-Fe/S for tetracycline adsorption and studies on-site energy distribution. Bioresour Technol. 2019;294:122152. https://doi.org/10.1016/j.biortech.2019.122152
- [26] Dai Y, Zhang K, Meng X, Li J, Guan X, Sun Q, et al. New use for spent coffee ground as an adsorbent for tetracycline removal in water. Chemosphere. 2019;215:163-72. https://doi.org/10.1016/j.chemosphere.2018.09.150
- [27] Li MF, Liu YG, Liu SB, Zeng GM, Hu XJ, Tan XF, et al. Performance of magnetic graphene oxide/diethylenetriamine penta acetic acid nanocomposite for the tetracycline and ciprofloxacin adsorption in single and binary systems. J Colloid Interface Sci. 2018;521:150-9. https://doi.org/10.1016/j.jcis.2018.03.003
- [28] Chen L, Yuan T, Ni R, Yue Q, Gao B. Multivariate optimization of ciprofloxacin removal by polyvinylpyrrolidone destabilized NZVI/Cu bimetallic particles. Chem Eng J. 2019;365:183-92. https://doi.org/10.1016/j.cej.2019.02.051
- [29] Selmi T, Sanchez-Sanchez A, Gadonneix P, Jagiello J, Seffen M, Sammouda H, et al. Tetracycline removal with activated carbons produced by hydrothermal carbonization of Agave americana fibers and mimosa tannin. Ind Crops Prod. 2018;115:146-57. https://doi.org/10.1016/j.indcrop.2018.02.005
- [30] Dutta V, Singh P, Shandilya P, Sharma S, Raizada P, Saini AK, et al. Review on advances in photocatalytic water disinfection utilizing graphene and graphene derivatives-based nanocomposites. J Environ Chem Eng. 2019;7:103132. https://doi.org/10.1016/j.jece.2019.103132
- [31] de Sousa DNR, Insa S, Mozeto AA, Petrovic M, Chaves TF, Fadini PS. Equilibrium and kinetic studies of the adsorption of antibiotics from aqueous solutions onto powdered zeolites. Chemosphere. 2018;205:137-46. https://doi.org/10.1016/j.chemosphere.2018.04.085

- [32] Premarathna KSD, Rajapaksha AU, Adassoriya N, Sarkar B, Sirimuthu NMS, Cooray A, et al. Clay-biochar composites for sorptive removal of tetracycline antibiotic in aqueous media. J Environ Manage. 2019;238:315-22. https://doi.org/10.1016/j.jenvman.2019.02.069
- [33] Beiranvand M, Farhadi S, Mohammadi A. Graphene oxide/hydroxyapatite/silver (rGO/HAP/Ag) nanocomposite: synthesis, characterization, catalytic and antibacterial activity. Int J Nano Dimens. 2019;10:180-94.
- [34] Xu Y, An L, Chen L, Xu H, Zeng D, Wang G. Controlled hydrothermal synthesis of strontium-substituted hydroxyapatite nanorods and their application as a drug carrier for proteins. Adv Powder Technol. 2018;29:1042-8. https://doi.org/10.1016/j.apt.2018.01.008
- [35] Jung KW, Lee SY, Choi JW, Lee YJ. A facile one-pot hydrothermal synthesis of hydroxyapatite/biochar nanocomposites: adsorption behavior and mechanisms for the removal of copper(II) from aqueous media. Chem Eng J. 2019;369:529-41. https://doi.org/10.1016/j.cej.2019.03.102
- [36] Kumar GS, Karunakaran G, Girija EK, Kolesnikov E, Van Minh N, Gorshenkov MV, et al. Size and morphology-controlled synthesis of mesoporous hydroxyapatite nanocrystals by microwave-assisted hydrothermal method. Ceram Int. 2018;44:11257-64. https://doi.org/10.1016/j.ceramint.2018.03.170
- [37] Syarif DG, Prajitno DH, Kurniawan A, Febrian MB, Lesmana R. Hydrothermally synthesis and characterization of HAP and Zr-doped HAP nanoparticles from bovine bone and zircon for photodynamic therapy. Process Appl Ceram. 2021;15:146-53. https://doi.org/10.2298/PAC2102146S
- [38] Sadat-Shojai M, Khorasani M, Dinpanah-Khoshdargi MT. Synthesis methods for nanosized hydroxyapatite with diverse structures. Acta Biomater. 2013;9:7591-621. https://doi.org/10.1016/j.actbio.2013.04.012
- [39] Monvisade P, Siriphannon P. Chitosan intercalated montmorillonite: Preparation, characterization and cationic dye adsorption. Appl Clay Sci. 2009;42:427-31. doi:10.1016/j.clay.2008.04.013. https://doi.org/10.1016/j.clay.2008.04.013
- [40] Parolo ME, Savini MC, Vallés JM, Baschini MT, Avena MJ. Tetracycline adsorption on montmorillonite: pH and ionic strength effects. Appl Clay Sci. 2008;40:179-86. https://doi.org/10.1016/j.clay.2007.08.003
- [41] Arora C, Kumar P, Soni S, Mittal J, Mittal A, Singh B. Efficient removal of malachite green dye from aqueous solution using Curcuma caesia based activated carbon. Desal Water Treat. 2020;195:341-52. https://doi.org/10.5004/dwt.2020.25897
- [42] Balarak D, Azarpira H. Rice husk as a biosorbent for antibiotic metronidazole removal: isotherm studies and model validation. Int J ChemTech Res. 2016;9:566-73. https://doi.org/10.21786/bbrc/9.3/32
- [43] Balarak D, Azarpira H, Mostafapour FK. Study of the adsorption mechanisms of cephalexin onto Azolla filiculoides. Pharm Chem. 2016;8:114-21.
- [44] Rivera-Utrilla J, Gomez-Pacheco CV, Sonchez-Polo M, Lopez-Peoalver JJ. Tetracycline removal from water by adsorption/bioadsorption on activated carbons and sludge-derived adsorbents. Environ Manage. 2013;131:16-24. https://doi.org/10.1016/j.jenvman.2013.09.024
- [45] Ji LL, Chen W, Duan L, Zhu DQ. Mechanisms for strong adsorption of tetracycline to carbon nanotubes: a comparative study using activated carbon and graphite as adsorbents. Environ Sci Technol. 2009;43:2322-7. https://doi.org/10.1021/es803268b
- [46] Tang Y, Guo H, Xiao L, Yu S, Gao N, Wang Y. Synthesis of reduced graphene oxide/magnetite composites and investigation of their adsorption performance of fluoroquinolone antibiotics. Colloids Surf A. 2013;424:74-80. https://doi.org/10.1016/j.colsurfa.2013.02.030
- [47] Abifarin JK, Obada DO, Dauda ET, Dodoo-Arhin D. Experimental data on the characterization of hydroxyapatite synthesized from biowastes. Data Brief. 2019;26:104485. https://doi.org/10.1016/j.dib.2019.104485
- [48] Bow SJ, Liou SZC, Chen SY. Structural characterization of room-temperature synthesized nano-sized β -tricalcium phosphate. Biomaterials. 2004;25:3155-61. https://doi.org/10.1016/j.biomaterials.2003.10.046
- [49] Kanan S, Ventura JMG, Lemos AF, Barba A, Ferreira JMF. Effect of sodium addition on the preparation of hydroxyapatites and biphasic ceramics. Ceram Int. 2008;34:7-13. https://doi.org/10.1016/j.ceramint.2006.07.007
- [50] Manso-Silva MN, Langlet M, Jiménez C, Fernández M, Martínez-Duarta JM. Calcium phosphate coatings prepared by aerosol-gel. J Eur Ceram Soc. 2003;23: pp.243-246. https://doi.org/10.1016/S0955-2219(02)00187-5